OXFORD

Human Molecular Genetics, 2018, Vol. 27, No. 5 811–822

doi: 10.1093/hmg/ddx442
Advance Access Publication Date: 2 January 2018
Original Article

ORIGINAL ARTICLE

Gaucher disease iPSC-derived osteoblasts have developmental and lysosomal defects that impair bone matrix deposition

Leelamma M. Panicker[1,†], Manasa P. Srikanth[1,†], Thiago Castro-Gomes[2], Diana Miller[1], Norma W. Andrews[2] and Ricardo A. Feldman[1,*]

[1]Department of Microbiology and Immunology, University of Maryland School of Medicine, Baltimore, MD 21201, USA and [2]Department of Cell Biology and Molecular Genetics, University of Maryland College Park, MD 20742, USA

*To whom correspondence should be addressed at: Department of Microbiology and Immunology, University of Maryland School of Medicine, 685 West Baltimore Street, HSF-1, Room 380, Baltimore, MD 21201, USA. Tel: +1 4107064198; Fax: +1 4107062129; Email: rfeldman@som.umaryland.edu

Abstract

Gaucher disease (GD) is caused by bi-allelic mutations in *GBA1*, the gene that encodes acid β-glucocerebrosidase (GCase). Individuals affected by GD have hematologic, visceral and bone abnormalities, and in severe cases there is also neurodegeneration. To shed light on the mechanisms by which mutant GBA1 causes bone disease, we examined the ability of human induced pluripotent stem cells (iPSC) derived from patients with Types 1, 2 and 3 GD, to differentiate to osteoblasts and carry out bone deposition. Differentiation of GD iPSC to osteoblasts revealed that these cells had developmental defects and lysosomal abnormalities that interfered with bone matrix deposition. Compared with controls, GD iPSC-derived osteoblasts exhibited reduced expression of osteoblast differentiation markers, and bone matrix protein and mineral deposition were defective. Concomitantly, canonical Wnt/β catenin signaling in the mutant osteoblasts was downregulated, whereas pharmacological Wnt activation with the GSK3β inhibitor CHIR99021 rescued GD osteoblast differentiation and bone matrix deposition. Importantly, incubation with recombinant GCase (rGCase) rescued the differentiation and bone-forming ability of GD osteoblasts, demonstrating that the abnormal GD phenotype was caused by GCase deficiency. GD osteoblasts were also defective in their ability to carry out Ca^{2+}-dependent exocytosis, a lysosomal function that is necessary for bone matrix deposition. We conclude that normal GCase enzymatic activity is required for the differentiation and bone-forming activity of osteoblasts. Furthermore, the rescue of bone matrix deposition by pharmacological activation of Wnt/β catenin in GD osteoblasts uncovers a new therapeutic target for the treatment of bone abnormalities in GD.

Introduction

Gaucher disease (GD) is an inherited autosomal recessive disorder with a carrier frequency of 1:18 among the Ashkenazi Jewish population and a disease incidence of 1:50 000 in the general population (1,2). GD is caused by mutations in the *GBA1* gene, which encodes lysosomal β glucocerebrosidase (GCase) (3,4). Patients with GD are generally classified into three clinical subtypes: Type 1 (non-neuronopathic), Type 2 (acute neuronopathic) and Type 3 (chronic neuronopathic), but there is great clinical variability between patients, suggesting that environmental factors and genetic background play

[†]These authors contributed equally to this work.

Received: October 3, 2017. **Revised:** December 20, 2017. **Accepted:** December 27, 2017

an important role in determining the course of the disease (5). GCase enzyme deficiency results in the accumulation of glucosylceramide, primarily in macrophages, owing to their inability to digest glucosylceramide present in the plasma membrane (PM) of phagocytosed red blood cells (6–8). This accumulation leads to the appearance of lipid-engorged, pathologic Gaucher macrophages in bone marrow, liver and spleen (9). Other clinical manifestations include anemia, thrombocytopenia and bone disease (3,5,10–13). In addition, 20% of GD cases involving severe mutations result in significant neuronopathy (14–17).

To model GD we generated induced pluripotent stem cells (iPSC) from patients with all three clinical subtypes of GD and differentiated them to cell types affected in the disease. GD iPSC-derived macrophages had a striking defect in clearance of phagocytosed red blood cells, recapitulating a pathologic hallmark of the disease (18); using hematopoietic progenitors derived from GD iPSC we found that mutant GCase causes developmental abnormalities in the hematopoietic lineage resulting in aberrant myelopoiesis and decreased erythropoiesis, reflecting the cytopenias in GD patients (19); we also found that iPSC-derived neurons from neuronopathic GD patients have reduced lysosomal biogenesis, dysregulated autophagy, and developmental defects, which may contribute to *GBA1*-associated neurodegeneration (20,21). All of the phenotypic abnormalities observed in GD macrophages, hematopoietic lineages and neuronal cells were reversed by recombinant GCase, demonstrating that the phenotypes observed were indeed caused by GCase deficiency and were not an artifact of the iPSC system.

Patients affected by all types of GD develop bone disease, and its manifestations include osteopenia, osteoporosis, reduced bone mineral density, increased fracture risk, avascular necrosis, bone infarctions and growth retardation in severe cases (22–26). Enzyme replacement therapy (ERT) with recombinant glucocerebrosidase reverses hematological and visceral parameters in Type 1 GD patients within 6 months (27). While the skeletal manifestations in GD are reversed more slowly by ERT, there is very significant reduction in osteopenia, in particular in young patients (25,28,29). The mechanisms leading to GD bone pathology are still unknown, but studies in animal models of GD with a targeted deletion of *GBA1* in the hemangioblast compartment have shown dysfunctional osteoblast activity resulting in decreased bone mineralization (30). Studies in zebrafish showed that *GBA1* loss of function is associated with impaired osteoblast differentiation and defective bone ossification, owing to increased oxidative stress and reduced Wnt/β-catenin signaling (31). It is also believed that increased osteoclast numbers in circulation and the inflammatory environment in GD are also important contributors to the bone pathology in this disorder (6,32–39).

In this study we used iPSC-derived osteoblasts from GD patients to identify the mechanisms leading to bone disease in these patients. We report that GD osteoblasts have developmental defects, as evidenced by their inability to fully differentiate into functional osteoblasts capable of normal bone deposition. We also found downregulation of Wnt/β-catenin signaling, which may contribute to the developmental defects of GD osteoblasts. In addition, the mutant osteoblasts had reduced numbers of lysosomes, there was a concomitant reduction in lysosomal hydrolases, and lysosomes from GD osteoblasts exhibited defective exocytosis, a process that is critical for deposition of bone matrix protein and mineral.

Results

Directed differentiation of GD iPSC to mesenchymal stem cells and osteoblasts

The control and GD iPSC used in this study have been previously described (6,18) and are listed in Supplementary Material, Table S1. Control and GD iPSC were differentiated to mesenchymal stem cells (MSC) via embryoid bodies followed by culture in osteogenic differentiation media as described in the section 'Materials and Methods'. The MSC were then analyzed for expression of specific markers by flow cytometry. Both control and GD iPSC were efficiently differentiated to MSC as determined by expression of CD44, CD29, HLA-ABC, and lack of expression of the hematopoietic marker CD45 (Fig. 1A; Supplementary Material, Fig. S1). More than 95% of control and GD MSC expressed markers of MSC.

Control and GD iPSC-derived MSC were then differentiated to osteoblasts by culturing in osteogenic media for 3 weeks, followed by mRNA analysis for expression of specific markers of osteoblast differentiation. As shown in Figure 1B and Supplementary Material, Figure S2A and B, GD osteoblasts expressed lower levels of alkaline phosphatase (ALP), Collagen 1 (Col1), and Runx2 mRNA than control cells. Osteocalcin was also downregulated in GD osteoblasts (data not shown). ALP is an enzyme secreted in vesicles into the extracellular space, where it hydrolyzes pyrophosphate and other phosphate moieties to monophosphate (40–42). This enzyme is critical for mineral bone matrix formation, whereas Col1 is a major component of the protein bone matrix (43,44). As shown in Figure 1C and Supplementary Material, Figure S2C, GD osteoblasts had very reduced levels of ALP enzymatic activity compared with controls. The ability of GD iPSC-osteoblasts to deposit mineral matrix as measured by Alizarin Red staining, was also considerably reduced compared with control osteoblasts (Fig. 1D).

GD osteoblasts expressed low levels of GCase compared with control osteoblasts (Fig. 2A). To determine whether the defects in osteoblast differentiation and mineral deposition could be reversed by treatment with recombinant GCase (rGCase), control and GD iPSC-derived MSC were differentiated in osteogenic media supplemented with rGCase enzyme throughout the 3-week differentiation period. As shown in Figure 2B and Supplementary Material, Figure S3, rGCase was able to restore ALP enzymatic activity and calcium phosphate deposition by GD osteoblasts, demonstrating that the phenotype observed was caused by GCase deficiency. The ability of rGCase to reverse the phenotype caused by even severe Types 2 and 3 GD mutations suggests that the recombinant enzyme can overcome the deleterious effects of a potential gain-of-function by mutant GCase.

Taken together, the reduction in markers of osteoblast differentiation and the defects in matrix protein and mineral deposition in the mutant cells suggest that GCase deficiency interferes with osteoblast differentiation and their bone-forming ability.

Downregulation of Wnt/β-catenin signaling in GD iPSC osteoblasts

As the canonical Wnt/β-catenin pathway plays a major role in osteoblast differentiation and maturation (45–48), we examined whether Wnt signaling was affected in the mutant osteoblasts. To this end, we carried out immunostaining for β-catenin, a major downstream mediator of Wnt signaling. Immunofluorescence

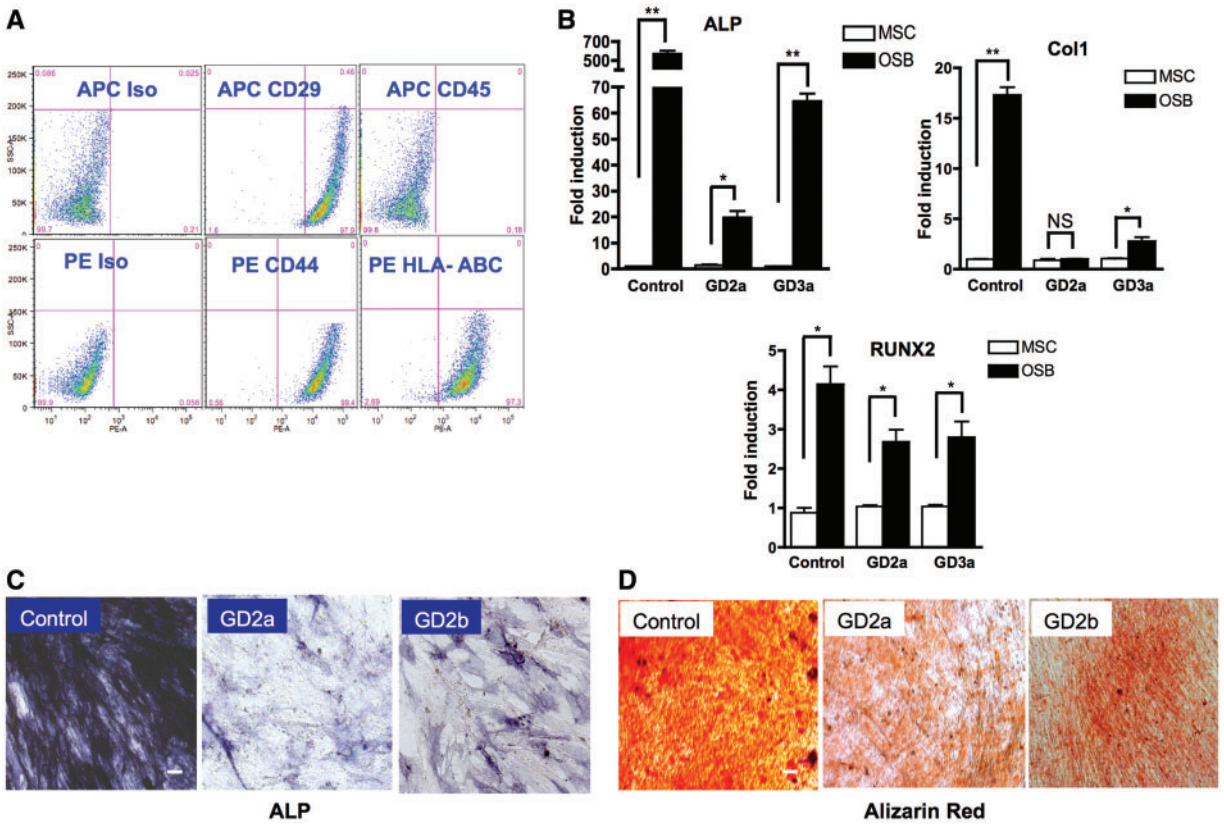

Figure 1. Characterization of mesenchymal stem cells and osteoblasts derived from control and GD iPSC. (**A**) Flow cytometry analysis of iPSC-derived control MSC. Scatter plots show staining for the specific markers of MSC, CD29, CD44 and HLA-ABC, and staining with anti-CD45 as a negative control. Isotype controls are shown at the left. (**B**) qRT-PCR analysis showing the expression of osteoblast markers in iPSC-derived control and GD MSC and osteoblasts as indicated. Results are expressed as fold-change of each osteoblast line compared with its corresponding MSC line (mean ± SEM). *P* values for control, GD2a and GD3a for each marker are as follows: ALP (0.003, 0.016 and 0.002), Col1 (0.002, 0.372 and 0.049), RUNX2 (0.020, 0.034 and 0.049). (**C**) Alkaline phosphatase stain in control and GD2 osteoblasts. (**D**) Alizarin red stain showing the mineral deposits in control and GD2 osteoblast cultures. Scale bar, 50 μm.

analysis showed decreased β-catenin levels in GD osteoblasts compared with those in control osteoblasts (Fig. 3A). Five-day incubation of GD osteoblasts with rGCase partially rescued total β-catenin levels in the mutant cells. To further assess the effect of mutant *GBA1* on Wnt/β-catenin signaling, we carried out immunofluorescence and immunoblot analysis using antibodies to the activated, unphosphorylated form of β-catenin. As shown in Figure 3B and C, GD osteoblasts had reduced levels of activated β-catenin, and rGCase treatment caused a significant increase in active β-catenin levels.

GSK3β, the major negative regulator of Wnt signaling, is a kinase that phosphorylates β-catenin, targeting it for degradation by the proteasome. The activity of GSK3β is negatively regulated by inhibitory phosphorylation on Ser 9 (49,50). To investigate the mechanism of β-catenin degradation in mutant osteoblasts, we examined expression of both total GSK3β and pGSK3β(S9). Western blot analysis showed no significant difference in total GSK3β protein level between control and mutant osteoblasts (Supplementary Material, Fig. S4A). However, there was a reduction in the levels of inhibitory pGSK3β(S9) in GD osteoblasts compared with controls (Supplementary Material, Fig. S4B). When differentiation of GD2 MSC to osteoblasts was carried out in the presence of rGCase the levels of pGSK3β(S9) were restored to control levels (Supplementary Material, Fig. S4B). Immunofluorescence images also showed reduced levels of pGSK3β(S9) in GD osteoblasts compared with control cells, and rescue by rGCase treatment (Supplementary Material, Fig. S4C). These data suggest that the reduced levels of β-catenin in GD osteoblasts may be a consequence of increased activity of GSK3β.

Taken together, our results suggest that GD osteoblasts have defective Wnt/β-catenin signaling, which may contribute to the defect in GD osteoblast differentiation we observed.

Pharmacological Wnt/β-catenin activation rescues GD osteoblast differentiation

To determine whether pharmacological activation of the Wnt/β-catenin pathway would restore GD osteoblast differentiation, we tested the effect of CHIR99021 (CHIR), a potent inhibitor of GSK3β (51). As shown in Supplementary Material, Figure S5, when we supplemented the osteogenic media with CHIR during differentiation of the mutant MSC to osteoblasts, this treatment restored ALP enzymatic activity and calcium phosphate deposition. These results suggest that downregulation of Wnt/β-catenin signaling by mutant GCase may be an important contributor to the developmental defects of GD osteoblasts. Furthermore, the functional rescue of GD osteoblasts by CHIR points to the Wnt pathway as a novel therapeutic target to treat the bone pathology in GD.

Lysosomal depletion in GD osteoblasts

As the deposition of bone matrix protein and minerals by osteoblasts is dependent on lysosomal functions such as exocytosis,

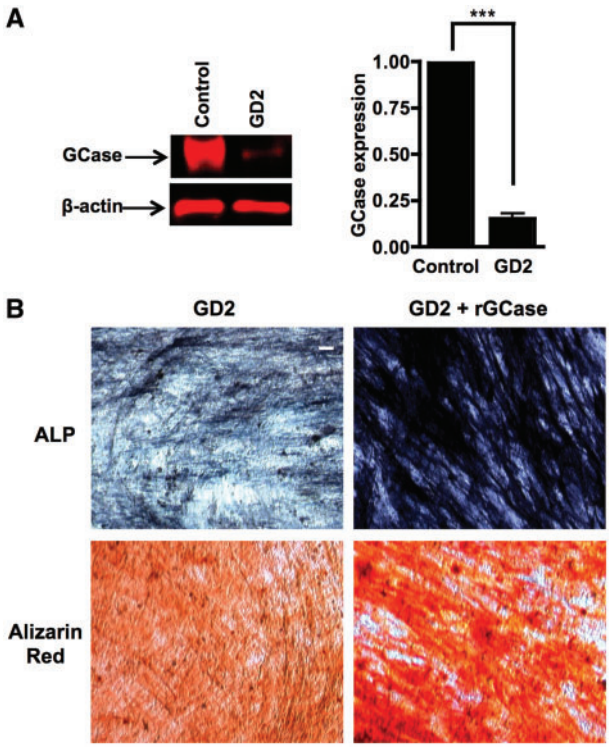

Figure 2. GCase expression in control and GD osteoblasts and phenotypic rescue by rGCase. (**A**) Left panel, representative immunoblot of GCase expression in control and GD2 iPSC-derived osteoblasts using specific antibodies to GCase. Right panel, quantitation of immunoblot analysis of GCase expression in control and GD2 osteoblasts. Results are expressed as fold-change compared with control osteoblasts ($n = 3$, ***$P < 0.001$). (**B**) GD2 iPSC-derived MSC were differentiated to osteoblasts in the absence or presence of 0.24 U/ml rGCase for 3 weeks. After differentiation, the cultures were stained for alkaline phosphatase (ALP) (upper panel) or Alizarin red (lower panel). Scale bar, 50 μm.

we assessed the integrity of the lysosomal compartment in GD osteoblasts. To this end, we first examined expression of lysosomal markers, and the activity of lysosomal hydrolases. Immunofluorescence analysis showed a reduction in expression of the lysosomal membrane protein LAMP1 in GD osteoblasts compared with control cells, and 5-day treatment of GD osteoblasts with rGCase restored LAMP1 expression to almost control levels (Fig. 4A and B). Immunoblot analysis also showed a reduction in LAMP1 protein levels in GD compared with control osteoblasts (Fig. 4C and D). In addition to lower expression of LAMP1, the enzymatic activities of the lysosomal hydrolases Cathepsin B, L, D and acid sphingomyelinase (ASM) in GD osteoblasts were reduced compared with those in control cells (Fig. 5A). These results show that mutant GCase has deleterious effects on the osteoblast lysosomal compartment and as shown below, this is reflected in an impairment of lysosomal exocytosis, a process that is required for bone deposition.

GD osteoblasts have defective lysosomal exocytosis

Regulated exocytosis is a Ca^{2+}-dependent process in which intracellular cytoplasmic vesicles fuse with the PM and release enzymes and other contents into the extracellular space (52–54). To assay for exocytosis, cells are treated with the pore-forming cytolysin streptolysin-O (SLO) in the presence of Ca^{2+}, which triggers a fusion of lysosomes with the PM, as part of a normal PM repair process. This process results in the release of lysosomal contents into the culture medium (55–57). To examine exocytosis in GD osteoblasts, control and GD osteoblasts were subjected to PM injury by treatment with SLO, and the activities of Cathepsins B, L and ASM were assayed as described in the section 'Materials and Methods'. As shown in Figure 5B, there was a decrease in Ca^{2+}-dependent exocytosis of Cathepsins B, L and ASM in GD osteoblasts compared with control cells. Taken together, our results showed that both, total Cathepsin and ASM activities (Fig. 5A) and exocytosed Cathepsin and ASM (Fig. 5B), were lower in GD osteoblasts than in control cells. To address whether the decrease of total hydrolase activity observed was the cause of lower exocytosed enzymatic activity, we calculated the exocytosis efficiency by normalizing exocytosed to total Cathepsin L. As shown in Figure 5C, lysosomal exocytosis in GD osteoblasts was defective, suggesting that the decrease in exocytosed protease activity was not secondary to the reduced total levels of hydrolases, but that it was caused by an intrinsic defect in exocytosis in the mutant cells. We then examined whether the exocytosis phenotype of the mutant osteoblasts would be rescued by rGCase. iPSC-derived MSC were differentiated in osteogenic media in the presence or absence of rGCase, and the cells were assayed for exocytosis. As shown in Supplementary Material, Figure S6, rGCase was able to significantly restore Cathepsin B exocytosis in the mutant osteoblasts.

We conclude that Ca^{2+}-dependent exocytosis, a lysosomal function that is critically required for bone matrix deposition, is significantly impaired by GCase deficiency.

Defective PM repair in GD iPSC osteoblasts

PM repair is a survival process that is constantly taking place in healthy cells and is regulated by Ca^{2+}-dependent exocytosis of lysosomal repair enzymes (55,58). As exocytosis in GD osteoblasts was compromised, we wanted to determine whether PM repair was also impaired. To examine the membrane repair ability of GD osteoblasts, GD and control cells were tested for their ability to repair membrane wounds made by the pore-forming toxin SLO, taking advantage of the membrane impermeant dye propidium iodide (PI). In the presence of Ca^{2+} cells are able to repair their wounds and exclude PI, but under no Ca^{2+} conditions cells remain permeabilized, as indicated by PI staining. The sensitivity to wounding and PM repair ability at different concentrations of SLO with and without Ca^{2+} were established in control experiments. As shown in Supplementary Material, Fig. S7, control and mutant osteoblasts were equally susceptible to SLO permeabilization (Supplementary Material, Fig. S7A and C) and the optimum concentration of SLO to achieve effective resealing in the presence of Ca^{2+} was 50 ng/ml (Supplementary Material, Fig. S7B and D). Therefore, this was the concentration used in the subsequent PM repair assays. Control and mutant cells were treated with SLO, stained with PI, and permeabilization was evaluated by flow cytometry. As shown in Figure 6A and B, in the absence of Ca^{2+}, both control and mutant osteoblasts exhibited the same PI staining with and without SLO. However, in the presence of Ca^{2+}, GD osteoblasts had a reduced ability to carry out PM repair compared with control cells (Fig. 6C). A similar defect in PM repair in the presence of Ca^{2+} was observed in GD osteoblasts mechanically injured by scraping of the dish (results not shown). Taken together, these results suggest that GCase deficiency causes significant alterations in the ability of GD osteoblasts to carry out Ca^{2+}-dependent exocytosis and PM repair, two lysosome-dependent

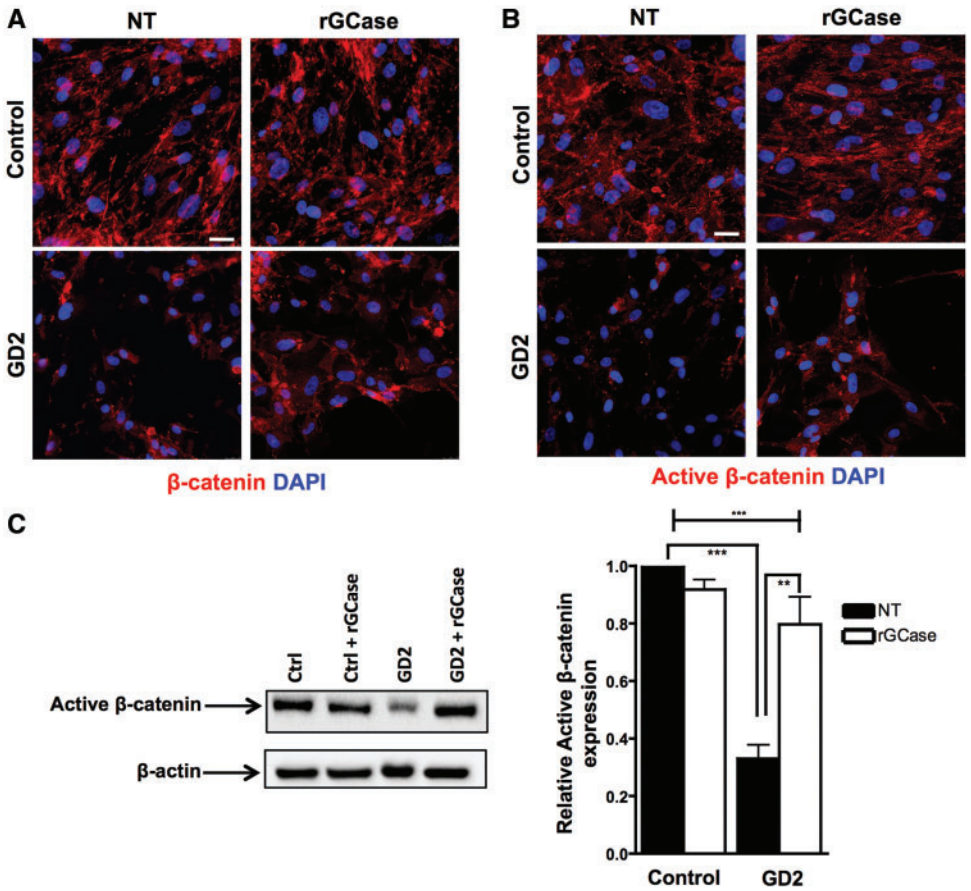

Figure 3. GD osteoblasts have lower levels of total and active β-catenin. (**A**) Control and GD2 iPSC-derived osteoblasts were incubated in the absence or presence of 0.24 U/ml rGCase for 5 days. The cultures were then stained using anti-β catenin antibody (red). Nuclei were stained with DAPI (blue). Magnification, ×40. Scale bar, 25 μm. (**B**) Control and GD2 osteoblasts were incubated in the absence or presence of 0.24 U/ml rGCase for 5 days. The cultures were then stained with antibodies to active β catenin (non-phosphorylated) (red). Nuclei were stained with DAPI (blue). Magnification, ×40. Scale bar, 25 μm. (**C**) Left panel, representative immunoblot showing the expression of active β catenin in control and GD2 osteoblasts that were incubated in the absence or presence of 0.24 U/ml rGCase. Right panel, quantitation of immunoblot analysis of active β catenin expression in control and GD2 osteoblasts; Results are expressed as fold-change with respect to non-treated control osteoblasts (mean ± SEM, $n = 3$). ***$P < 0.001$ (one-way ANOVA). ***$P < 0.001$ between control versus GD2, **$P < 0.01$ between GD2 versus GD2 + rGCase.

functions that are important for bone matrix deposition and osteoblast survival.

Discussion

In this study, we report that iPSC-derived osteoblasts from patients with GD have developmental defects and lysosomal functional abnormalities that interfere with their bone-forming ability. While GD iPSC differentiated normally to MSC, there was a substantial impairment in osteoblastic differentiation. GD iPSC osteoblasts exhibited lower levels of osteoblast markers including ALP, Col1 and Runx2, and there was a decrease in ALP enzymatic activity and calcium phosphate deposition. We found that Wnt/β-catenin signaling was downregulated in GD osteoblasts, and that pharmacologic Wnt activation rescued osteoblast differentiation. In addition to developmental defects, the mutant cells had reduced numbers of lysosomes, which were functionally deficient in their ability to carry out exocytosis and PM repair. Our results lend support to the idea that normal GCase activity plays an essential role in the ability of osteoblasts to carry out bone deposition, and further suggest that the *in vitro* phenotypes we observed contribute to the skeletal abnormalities seen in GD patients.

Patients with Type 1 GD may present with decreased bone density, osteoporosis, increased risk of bone fracture, bone crisis and osteonecrosis, and in Types 2 and 3 GD there is growth retardation (23,25). The etiology of the skeletal pathology in GD is not well understood. Maintenance of bone density and integrity is the result of a dynamic interaction between osteoblasts and osteoclasts (59,60). Osteoblasts, the cells primarily responsible for bone matrix deposition, secrete Type I Collagen, growth factors and calcium phosphate mineral complexes, which provide a strong and flexible bone structure. Osteoclasts, which are derived from myeloid hematopoietic progenitors, carry out bone resorption, secreting proteases that digest protein matrix, and protons that dissolve bone minerals (38). There is *in vivo* evidence that dysfunctional osteoblasts play a major role in GD bone disease. Using a mouse model in which the Mx1 promoter was used for targeted deletion of *GBA1* in hematopoietic and mesenchymal progenitors, Mistry *et al.* showed recapitulation of nearly all of the visceral abnormalities of Type 1 GD. The striking bone abnormalities observed were caused mainly by dysfunctional osteoblasts, while no major contributions from the bone-resorption activity of osteoclasts were reported (30).

To investigate whether GD iPSC-derived osteoblasts have developmental defects, we examined the ability of GD iPSC to

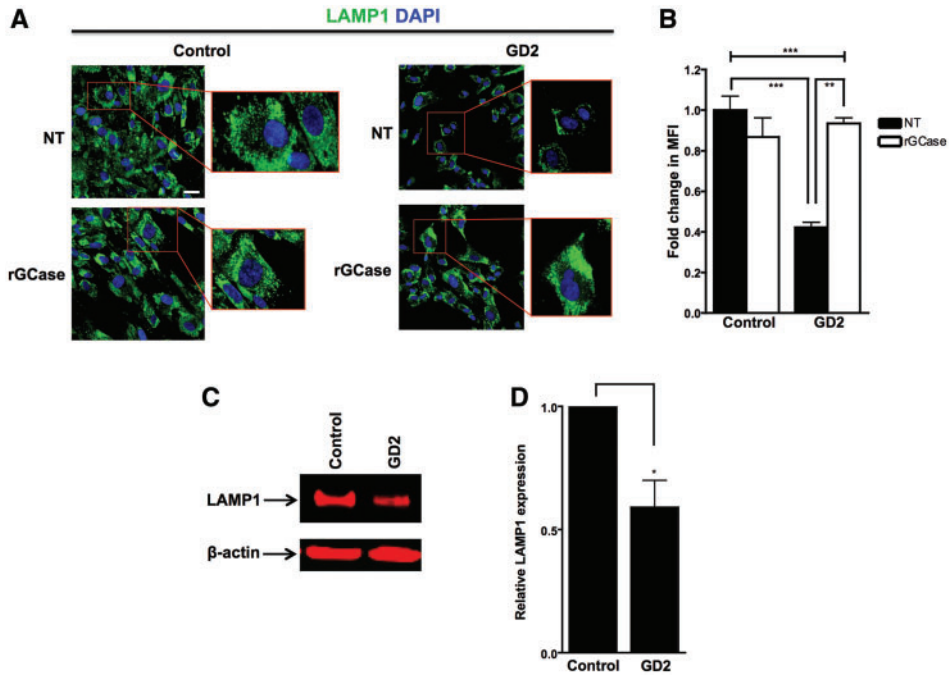

Figure 4. Lysosomal depletion in GD osteoblasts and rescue by rGCase. (**A**) Control and GD2 osteoblasts were incubated in the absence (NT) or presence of 0.24 U/ml rGCase for 5 days. The cultures were then stained with anti-LAMP1 antibody (green). Nuclei were stained with DAPI (blue). Magnification, ×40. Scale bar, 25 μm. (**B**) Quantitation of mean fluorescence intensity (MFI) of LAMP1 expression in control and GD2 osteoblasts. Results are expressed as fold-change with respect to non-treated control osteoblasts (mean ± SEM, $n = 3$). ***$P < 0.001$ (one-way ANOVA). ***$P < 0.001$ between control versus GD2, **$P < 0.01$ between GD2 versus GD2 + rGCase. (**C**) Representative immunoblot showing the expression of LAMP1 in control and GD2 osteoblasts. (**D**) Quantitation of immunoblot analysis of LAMP1 expression in control and GD2 osteoblasts; results are expressed as fold-change compared with control osteoblasts (mean ± SEM, $n = 3$, *$P < 0.05$).

differentiate to functional osteoblasts. While mutant GCase had no effect on the generation of MSC from GD iPSC, further differentiation under osteogenic conditions showed that mRNA levels of the osteoblast markers ALP and Col1 were reduced, suggesting that the differentiation of GD osteoblasts from MSC was compromised. Further analysis showed that GD osteoblasts had lower levels of total and activated β catenin, a major effector of the canonical Wnt/β-catenin pathway, and that excess β catenin degradation may be the result of increased GSK3β kinase activity. As the canonical Wnt pathway is an important regulator of osteoblast differentiation, our results suggest that mutant GCase may interfere with differentiation to mature osteoblasts in part through downregulation of Wnt/β catenin signaling. This conclusion is supported by the reversal of GD osteoblast phenotype by pharmacologic Wnt activation with CHIR, a potent inhibitor of GSK3β. Importantly, differentiation of MSC to osteoblasts in the continued presence of rGCase rescued GD osteoblast differentiation, demonstrating that the intrinsic developmental defects of GD osteoblasts observed were caused by GCase deficiency. Our results are in agreement with previous studies carried out in a zebrafish model of GD (31). In this system, a truncation in GCase that abolished its enzymatic activity resulted in bone abnormalities and defects in the Wnt/β-catenin pathway. Significantly, neuronopathic mutations in *GBA1* have been recently found to cause neurodevelopmental defects by interference with Wnt/β-catenin signaling (21). Thus, downregulation of this pathway may be a common mechanism by which mutant *GBA1* interferes with normal development in affected tissues. Future analysis will identify the precise mechanisms by with mutant GCase impairs Wnt/β-catenin signaling, and how this contributes to the developmental defects observed. GD osteoblasts also had lower levels of Runx2, another transcription factor important for osteoblast differentiation (61), suggesting that mutant GCase may interfere with osteoblast differentiation by more than one mechanism. Taken together, the results from this study, those of our previous work showing that GD hematopoietic and neuronal progenitors have intrinsic developmental defects (19,21), and recent reports from animal models (30,31,62–64), strongly suggest that mutant *GBA1* interferes with normal developmental pathways in a number of cell types affected in GD.

There is considerable evidence that *GBA1* deficiency disrupts the lysosomal compartment. In neurons, mutant GCase interferes with lysosomal biogenesis, there is accumulation of autophagic vesicles that are unable to fuse with lysosomes (20,65–68), and there is an increase in aggregate-prone proteins such as α-synuclein (66,69). This study showed that GD osteoblasts had reduced numbers of lysosomes, which were defective in their ability to carry out exocytosis, a process that is essential for the transport of bone matrix protein and mineralization enzymes to the extracellular space. Taken together, our results suggest that the impaired bone-forming activity of GD osteoblasts resulted from a combination of incomplete differentiation and impaired lysosomal function, and that the abnormalities identified in this iPSC system are likely to play a role in the skeletal manifestations in GD patients.

ERT with rGCase, which is successfully used to treat GD1 (27), corrects hepato-splenomegalia within 6 months. Although normalization of bone parameters by ERT takes longer, this treatment results in significant reversal of osteopenia, in particular in younger patients (29), and the risk of osteonecrosis is reduced. In GD patients treated by ERT, the infused enzyme is removed from circulation within minutes (70). This rapid uptake, mostly by liver parenchyma and Gaucher macrophages,

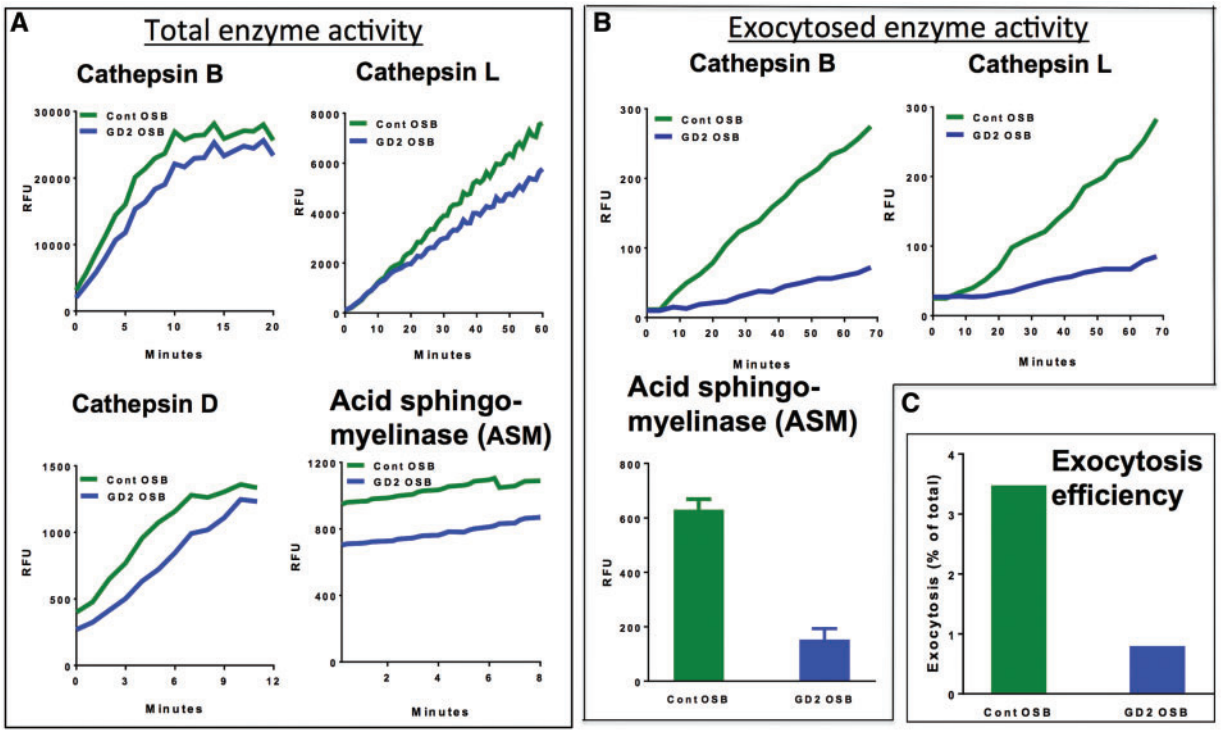

Figure 5. Reduced lysosomal enzyme activity and exocytosis in GD osteoblasts. (**A**) Cell lysates from control (green) and GD2 osteoblasts (blue) were assayed for activity of the lysosomal enzymes Cathepsins B, L, D and acid sphingomyelinase (ASM) as described in the section 'Materials and Methods'. Plots represent total enzymatic activities in control and GD2 osteoblasts. (**B**) Lysosomal exocytosis of Cathepsins B, L and ASM in SLO-permeabilized control and GD2 osteoblasts. Control and GD2 osteoblasts were treated with SLO, and the activities of Cathepsins B, L and ASM (mean ± SEM, $n = 3$, $^{**}P < 0.01$) in the supernatant were assayed as described in the section 'Materials and Methods'. Green, control osteoblasts; blue, GD2 osteoblasts. RFU, relative fluorescence units. (**C**) Exocytosis efficiency for Cathepsin L in control and GD2 osteoblasts was measured and expressed as the percentage of total Cathepsin L activity present in whole cell lysates of each cell type, as described in the section 'Materials and Methods'. Green, control osteoblasts; blue, GD2 osteoblasts. The results show that after SLO permeabilization, GD2 osteoblasts have defective Ca^{2+}-dependent lysosomal exocytosis.

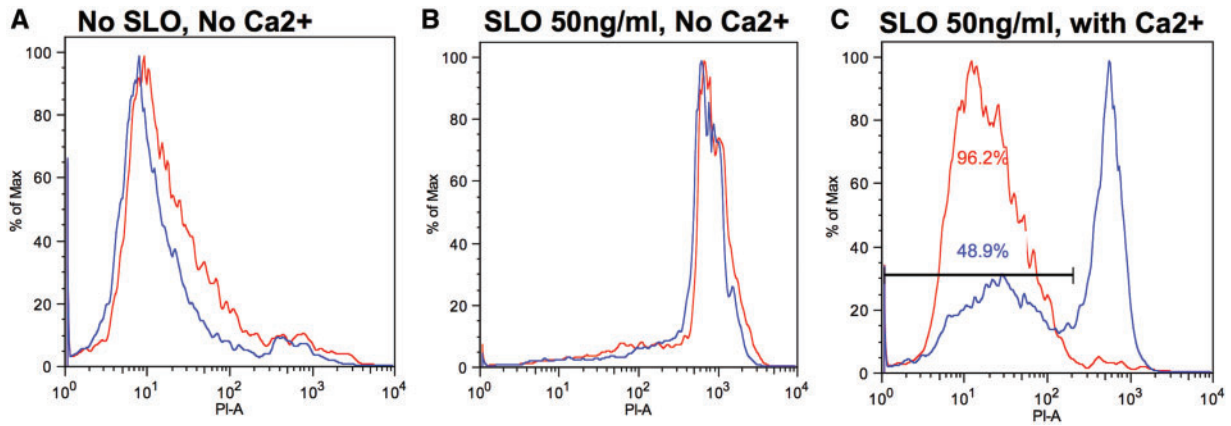

Figure 6. GD osteoblasts exhibit defective plasma membrane repair. Untreated and SLO-treated control and GD2 osteoblasts were incubated in the presence or absence of Ca^{2+} as described in the section 'Materials and Methods', and the samples were analyzed by FACS. (**A**) Cells without SLO and without Ca^{2+}. (**B**) Cells with SLO and without Ca^{2+}. (**C**) Membrane repair in the presence of both SLO and Ca^{2+}. Red, control osteoblasts; blue GD2 osteoblasts. In the assay shown, which is representative of several independent experiments, the extent of membrane repair was 48.9% in GD osteoblasts, and 96.2% in control osteoblasts.

may be one of the reasons that normalization of bone parameters is slower than reversal of visceral abnormalities caused by GCase deficiency. Our results showed that rGCase was very effective in rescuing bone deposition by GD osteoblasts, suggesting that targeting of rGCase to osteoblasts by improvements in enzyme delivery (71), would be of clinical benefit to treat the bone abnormalities in GD. Cerezyme, the enzyme preparation used in this study is an rGCase treated with glycosidases to expose mannose residues on its surface, which facilitates rGCase uptake by mannose receptors on Gaucher macrophages. Osteoblasts are not believed to have mannose receptors but they have mannose-6-phosphate (M6P) receptors (72). As Cerezyme also has exposed M6P (73), binding of this moiety to its receptor might mediate rGCase entry into osteoblasts.

However, preincubation of control or mutant osteoblasts with either mannan, a polymer of mannose, or with M6P, did not block rGCase uptake by these cells (data not shown), suggesting that rGCase was not taken up by iPSC osteoblasts through either mannose or M6P receptors. The important question of the mechanism of rGCase uptake by GD osteoblasts will be examined in future studies. Substrate reduction therapy, used as an alternative to ERT for treatment of Type 1 GD, also improves skeletal manifestations of GD over time (74–77). The results of our study showing that pharmacologic Wnt activation can rescue bone matrix deposition by GD osteoblasts, suggest that the Wnt pathway may be a novel druggable target to treat the bone pathology in GD. Although the pleiotropic effects of the Wnt pathway caution about potential side effects of Wnt modulators (78), some of these agents are now reaching the clinic. Romosozumab, a monoclonal antibody to the bone-specific Wnt antagonist sclerostin, is being evaluated in clinical trials for osteoporosis (79–81).

In summary, using a GD iPSC system, we found that GD osteoblasts have developmental defects, which may result from interference of mutant GCase with canonical Wnt/β-catenin signaling. Critical lysosomal functions such as Ca^{2+}-dependent exocytosis were also affected by GCase deficiency, and the net result was a greatly reduced deposition of bone matrix protein and mineral. Our results lend support to the idea that the defective phenotype of GD osteoblasts is likely to contribute to the bone manifestations observed in GD patients and animal models of GD. This study also points to the canonical Wnt signaling pathway as a novel therapeutic target to treat the skeletal abnormalities caused by GD.

Materials and Methods

iPSC lines

The iPSC from patients with Types 1, 2 and 3 GD (GD1a, GD1b, GD2a, GD2b, GD3a and GD3b), and from control subjects used in this study have been previously described (6,18) and are listed in Supplementary Material, Table S1. Their genotypes are: N370S/N370S (GD1a and GD1b), L444P/RecNciI (GD2a), W184/D409H (GD2b), L444P/L444P (GD3a and GD3b) and wild-type/wild-type (control MJ).

Generation of multipotent GD iPSC MSC

For embryoid body (EB) formation, iPSC were detached from plates and feeder cells by treatment with 0.2% dispase. The iPSC were transferred into 6-well, ultra-low attachment plates (Costar) and cultured for 10 days at 37°C in EB culture medium [DMEM-F12 (Invitrogen), 20% (v/v) Knockout Serum Replacement (Invitrogen), NEAA, 1 mM L-glutamine and 0.1 mM β-mercaptoethanol]. To initiate MSC differentiation, EBs were transferred to culture plates coated with 0.1% (w/v) gelatin and maintained in MSC culture medium [high glucose DMEM (Invitrogen), 20% FBS (Hyclone), 1 mM L-glutamine and 100 U/ml Pen/Strep (Invitrogen)]. Stromal cells surrounding the flattened EBs were visible after 3 days in adherent culture. Media was changed every other day for 10–15 days, and the cells were expanded in MSC media at 50% confluency. Cells were cultured for five passages, at which stage the MSC cultures had uniform morphology and expressed MSC-specific markers. MSC were then either differentiated to osteoblasts or cryopreserved until use.

Differentiation of GD iPSC-MSC to osteoblasts

iPSC-derived MSC were seeded on culture plates at 2×10^4 cells/cm^2) in MSC media. A day after seeding, cells were cultured in osteoblast differentiation media [MSC media supplemented with 10 mM beta-glycerophosphate (Sigma), 100 μM dexamethasone (Sigma) and 50 μg/ml ascorbic acid (Sigma)]. Media was changed every other day and cells were passaged upon attaining 90% confluency. The cells were cultured in osteoblast media for 3–4 weeks.

Antibodies

Markers for MSC characterization were APC- or FITC-conjugated anti-mouse anti-CD44 (Cat No. 550989), anti-CD29 (Cat No. 559883), anti-HLA-ABC (Cat No. 560168) and anti-CD45 (Cat No. 550566) from BD Bioscience (San Jose, CA, USA). The primary antibodies used for immunofluorescence and Western blotting were: LAMP1 (H4A3, University of Iowa Developmental Hybridoma Bank); GSK3β (Cat No. 12456), pGSK3β-Ser9 (Cat No.9323) and non-phospho (Active) β-catenin (Cat No. 8814) were from Cell Signaling; GBA1 (Cat No. WH0002629M1, Sigma); total β-catenin (Cat No. sc-7199, Santa Cruz). The secondary antibodies DyLight 488- or 549-conjugated mouse or rabbit immunoglobulin-specific antibodies were from Jackson InmmunoResearch Laboratories (West Grove).

Flow cytometry for marker analysis

iPSC-derived MSC were fixed in 4% paraformaldehyde, washed, and incubated in blocking buffer consisting of phosphate-buffered saline (PBS), human IgG (1 mg/ml, Sigma), 8% FBS and 0.01% sodium azide. Cells were then incubated with the indicated antibodies in buffer containing PBS, 0.2% saponin, 8% FBS and 0.01% sodium azide, washed, and kept at 4°C until FACS analysis. Data were acquired by flow cytometry using a BD LSRII Flow cytometer and analyzed using Flowjo software (Tree Star Inc., Ashland, OR).

Real time PCR

Control and GD iPSC-derived MSC in 12-well plates were cultured in osteoblast differentiation media for 3 weeks in duplicate wells. mRNA was isolated using a Qiagen kit, and cDNA was synthesized using the iScript kit (Bio-Rad). Gene expression quantification was achieved by qPCR (7900 HT: Applied Biosystems) using the SYBR Green method. The relative mRNA expression of each gene tested was normalized to the values of GAPDH mRNA for each reaction. The primers used are listed in Supplementary Material, Table S2.

Alizarin red stain

Control and GD iPSC-derived MSC were differentiated to osteoblasts on chamber slides for 21 days. Staining for mineral deposit was done using Alizarin red 0.5% (v/v) aqueous solution adjusted to pH 4.3 (Sigma), for half an hour at room temperature, followed by 3 washes with water. The chambers were removed and slides were allowed to dry.

ALP stain

Control and GD iPSC-derived MSC were differentiated to osteoblasts on chamber slides for 21 days and stained for ALP using a

SigmaFast BCIP/NBT tablet (Sigma Cat No. B5655) dissolved in water for 10 min at 37°C.

Immunocytochemistry

For marker expression analysis, osteoblasts were plated on chamber slides for 4–5 days. Cells were fixed in 4% paraformaldehyde, blocked (8% FBS in PBS) and incubated for 1 h with the indicated primary antibodies or matching isotype controls, followed by 1 h incubation with secondary antibodies. Cell nuclei were labeled using DAPI-containing mounting medium (Vectashield: Vector Laboratories Cat No. H-1200).

Recombinant GCase treatment

Recombinant human GCase (rGCase) (Cerezyme®, Genzyme, Cambridge, MA, USA) was added to the cultures at a concentration of 0.24 U/ml for the indicated times, and replenished with each media change. Cerezyme was obtained from patient infusion remnants.

PM injury and repair assay

iPSC osteoblasts were seeded at 5×10^5 cells/100 mm dish. After 48 h, cells were trypsinized and 1×10^5 cells/ml/treatment were used to perfom SLO wounding and PM repair assays. For cytolysin binding, cells were incubated with different concentrations of SLO (50, 100 and 150 ng/ml) for 5 min on ice. This step allows for cytolysin binding without causing pore formation. To induce pore formation and trigger PM repair, the cells were transferred to a 37°C water bath for 5 min. Experiments were done in the presence of Ca^{2+} for assessing PM repair, or without Ca^{2+} to assess the extent of SLO wounding. After 5 min at 37°C the cells were placed on ice for 2 min, followed by the addition of 50 μg/ml PI. The cell population was then analyzed by flow cytometry to measure the extent of PM repair; 1×10^4 cells were analyzed for each condition.

Exocytosis of lysosomal enzymes

For exocytosis assays, cells were seeded at 1×10^6 cells/35 mm dish in triplicate for each condition. After 24 h, the dishes were washed twice with chilled Ca^{2+}-free PBS and incubated with SLO (a high dose of 500 ng/ml was used to obtain maximum exocytosis) in the same buffer for 5 min on ice. The cells were then washed with the same media, transferred to a 37°C water bath, and 250 μl of 37°C pre-warmed Ca^{2+}-containing PBS were simultaneously added to the cell layer, to trigger pore formation and PM repair. After 5 s, the media containing the exocytosed lysosomal enzymes was recovered, chilled on ice and centrifuged at 200*g* to remove any detached cells. The supernatant was used to measure the activity of exocytosed lysosomal enzymes. To keep the assay time constant for each sample, transfer to the water bath was done one dish at a time. To assess exocytosis efficiency, the results were expressed as a percentage of the total activity of each enzyme present in the cell lysates. The samples were analyzed for enzyme activity using specific fluorimetric kits for the detection of Cathepsin B (ABCAM Cat. #ab65300), Cathepsin L (ABCAM Cat. #ab65306), Cathepsin D (ABCAM Cat. #ab65302) and ASM (Invitrogen Cat. #A12220) following the manufacturer's instructions. Cleavage of the fluorogenic specific substrates was monitored for up to 2 h in an ELISA reader as a measure of enzymatic activity, with the initial maximum velocity calculated from the slope of each reaction.

Western blot analysis

Cells were lysed directly in SDS sample buffer and analyzed by Western blot using specific antibodies as previously described (18).

Statistical analysis

Data were analyzed using Prism software version 4.0c (GraphPad Software). The significance of differences was assessed using two-tailed unpaired Student's *t*-tests or one-way ANOVA followed by Tukey Post post hoc test to compare different groups, as appropriate. The confidence level for significance was 95%.

Supplementary Material

Supplementary Material is available at *HMG* online.

Conflict of Interest statement: None declared.

Funding

This work was supported by grants from the Maryland Stem Cell Research Fund (MSCRF) 2009-MSCRFII-0082-00 (RAF), a UMB/UMCP Research Seed Program Grant (RAF and NWA), and NIH R01 GM064625 (NWA).

References

1. Grabowski, G.A., Petsko, G.A., Kolodny, E.H. (2014) Gaucher Disease. In Valle, D., Beaudet, A.L., Vogelstein, B., Kinzler, K.W., Antonarakis, S.E., Ballabio, A., Gibson, K., Mitchell, G. (eds.), *The Metabolic and Molecular Bases of Inherited Disease*. McGraw-Hill, New York, pp. 3635–3668.
2. Tsuji, S., Martin, B.M., Barranger, J.A., Stubblefield, B.K., LaMarca, M.E. and Ginns, E.I. (1988) Genetic heterogeneity in type 1 gaucher disease: multiple genotypes in ashkenazic and non-ashkenazic individuals. *Proc. Natl. Acad. Sci. USA.*, **85**, 2349–2352.
3. Cox, T.M. (2010) Gaucher disease: clinical profile and therapeutic developments. *Biologics*, **4**, 299–313.
4. Brady, R.O., Kanfer, J.N., Bradley, R.M. and Shapiro, D. (1966) Demonstration of a deficiency of glucocerebroside-cleaving enzyme in Gaucher's disease. *J. Clin. Invest.*, **45**, 1112–1115.
5. Sidransky, E. (2012) Gaucher disease: insights from a rare Mendelian disorder. *Discov. Med.*, **14**, 273–281.
6. Panicker, L.M., Miller, D., Awad, O., Bose, V., Lun, Y., Park, T.S., Zambidis, E.T., Sgambato, J.A. and Feldman, R.A. (2014) Gaucher iPSC-derived macrophages produce elevated levels of inflammatory mediators and serve as a new platform for therapeutic development. *Stem Cells*, **32**, 2338–2349.
7. Mignot, C., Gelot, A. and De Villemeur, T.B. (2013) Gaucher disease. *Handb. Clin. Neurol.*, **113**, 1709–1715.
8. Messner, M.C. and Cabot, M.C. (2010) Glucosylceramide in humans. *Adv. Exp. Med. Biol.*, **688**, 156–164.
9. Machaczka, M., Klimkowska, M., Regenthal, S. and Hagglund, H. (2011) Gaucher disease with foamy transformed macrophages and erythrophagocytic activity. *J. Inherit. Metab. Dis.*, **34**, 233–235.
10. Cox, T.M. and Schofield, J.P. (1997) 3 gaucher's disease: clinical features and natural history. *Baillière's Clin. Haematol.*, **10**, 657–689.
11. Dandana, A., Ben Khelifa, S., Chahed, H., Miled, A. and Ferchichi, S. (2016) Gaucher disease: clinical, biological and therapeutic aspects. *Pathobiology*, **83**, 13–23.

12. Brady, R.O., Kanfer, J.N. and Shapiro, D. (1965) Metabolism of glucocerebrosides. ii. evidence of an enzymatic deficiency in gaucher's disease. *Biochem. Biophys. Res. Commun.*, **18**, 221–225.
13. Thomas, A.S., Mehta, A. and Hughes, D.A. (2014) Gaucher disease: haematological presentations and complications. *Br. J. Haematol.*, **165**, 427–440.
14. Vitner, E.B. and Futerman, A.H. (2013) Neuronal forms of gaucher disease. *Handb. Exp. Pharmacol.*, **216**, 405–419.
15. Sidransky, E. (2004) Gaucher disease: complexity in a "simple" disorder. *Mol. Genet. Metab.*, **83**, 6–15.
16. Farfel-Becker, T., Vitner, E.B., Pressey, S.N., Eilam, R., Cooper, J.D. and Futerman, A.H. (2011) Spatial and temporal correlation between neuron loss and neuroinflammation in a mouse model of neuronopathic gaucher disease. *Hum. Mol. Genet.*, **20**, 1375–1386.
17. Wong, K., Sidransky, E., Verma, A., Mixon, T., Sandberg, G.D., Wakefield, L.K., Morrison, A., Lwin, A., Colegial, C., Allman, J.M. *et al.* (2004) Neuropathology provides clues to the pathophysiology of gaucher disease. *Mol. Genet. Metab.*, **82**, 192–207.
18. Panicker, L.M., Miller, D., Park, T.S., Patel, B., Azevedo, J.L., Awad, O., Masood, M.A., Veenstra, T.D., Goldin, E., Stubblefield, B.K. *et al.* (2012) Induced pluripotent stem cell model recapitulates pathologic hallmarks of gaucher disease. *Proc. Natl. Acad. Sci. USA.*, **109**, 18054–18059.
19. Sgambato, J.A., Park, T.S., Miller, D., Panicker, L.M., Sidransky, E., Lun, Y., Awad, O., Bentzen, S.M., Zambidis, E.T. and Feldman, R.A. (2015) Gaucher disease-induced pluripotent stem cells display decreased erythroid potential and aberrant myelopoiesis. *Stem Cells Transl. Med.*, **4**, 878–886.
20. Awad, O., Sarkar, C., Panicker, L.M., Miller, D., Zeng, X., Sgambato, J.A., Lipinski, M.M. and Feldman, R.A. (2015) Altered TFEB-mediated lysosomal biogenesis in gaucher disease iPSC-derived neuronal cells. *Hum. Mol. Genet.*, **24**, 5775–5788.
21. Awad, O., Panicker, L.M., Deranieh, R.M., Srikanth, M.P., Brown, R.A., Voit, A., Peesay, T., Park, T.S., Zambidis, E.T. and Feldman, R.A. (2017) Altered differentiation potential of gaucher's disease iPSC neuronal progenitors due to wnt/beta-catenin downregulation. *Stem Cell. Rep.*, **9**, 1853–1867.
22. Bembi, B., Ciana, G., Mengel, E., Terk, M.R., Martini, C. and Wenstrup, R.J. (2002) Bone complications in children with gaucher disease. *Br. J. Radiol.*, **75**, A37–A44.
23. Elstein, D., Itzchaki, M. and Mankin, H.J. (1997) Skeletal involvement in gaucher's disease. *Baillieres Clin. Haematol.*, **10**, 793–816.
24. Giuffrida, G., Cingari, M.R., Parrinello, N., Romano, A., Triolo, A., Franceschino, M. and Di Raimondo, F. (2012) Bone turnover markers in patients with type 1 gaucher disease. *Hematol. Rep.*, **4**, 70–79.
25. Goker-Alpan, O. (2011) Therapeutic approaches to bone pathology in gaucher disease: past, present and future. *Mol. Genet. Metab.*, **104**, 438–447.
26. Biegstraaten, M., Cox, T.M., Belmatoug, N., Berger, M.G., Collin-Histed, T., Vom Dahl, S., Rocco Fraga, D.M., Giona, C., Giraldo, F., P. *et al.* (2016) Management goals for type 1 gaucher disease: an expert consensus document from the European working group on gaucher disease. *Blood Cells Mol. Dis.*, **68**, 203–208.
27. Brady, R.O. (2006) Enzyme replacement for lysosomal diseases. *Annu. Rev. Med.*, **57**, 283–296.
28. Elstein, D., Foldes, A.J., Zahrieh, D., Cohn, G.M., Djordjevic, M., Brutaru, C. and Zimran, A. (2011) Significant and continuous improvement in bone mineral density among type 1 gaucher disease patients treated with velaglucerase alfa: 69-month experience, including dose reduction. *Blood Cells Mol. Dis.*, **47**, 56–61.
29. Mistry, P.K., Weinreb, N.J., Kaplan, P., Cole, J.A., Gwosdow, A.R. and Hangartner, T. (2011) Osteopenia in gaucher disease develops early in life: response to imiglucerase enzyme therapy in children, adolescents and adults. *Blood Cells Mol. Dis.*, **46**, 66–72.
30. Mistry, P.K., Liu, J., Yang, M., Nottoli, T., McGrath, J., Jain, D., Zhang, K., Keutzer, J., Chuang, W., Mehal, W.Z. *et al.* (2010) Glucocerebrosidase gene-deficient mouse recapitulates gaucher disease displaying cellular and molecular dysregulation beyond the macrophage. *Proc. Natl. Acad. Sci. USA.*, **107**, 19473–19478.
31. Zancan, I., Bellesso, S., Costa, R., Salvalaio, M., Stroppiano, M., Hammond, C., Argenton, F., Filocamo, M. and Moro, E. (2015) Glucocerebrosidase deficiency in zebrafish affects primary bone ossification through increased oxidative stress and reduced wnt/beta-catenin signaling. *Hum. Mol. Genet.*, **24**, 1280–1294.
32. Allen, M.J., Myer, B.J., Khokher, A.M., Rushton, N. and Cox, T.M. (1997) Pro-inflammatory cytokines and the pathogenesis of gaucher's disease: increased release of interleukin-6 and interleukin-10. *QJM*, **90**, 19–25.
33. Barak, V., Acker, M., Nisman, B., Kalickman, I., Abrahamov, A., Zimran, A. and Yatziv, S. (1999) Cytokines in gaucher's disease. *Eur. Cytokine Netw.*, **10**, 205–210.
34. Fierro, F.A., Nolta, J.A. and Adamopoulos, I.E. (2017) Concise review: stem cells in osteoimmunology. *Stem Cells*, **35**, 1461–1467.
35. Hong, Y.B., Kim, E.Y. and Jung, S.C. (2006) Upregulation of proinflammatory cytokines in the fetal brain of the gaucher mouse. *J. Korean Med. Sci.*, **21**, 733–738.
36. Moran, M.T., Schofield, J.P., Hayman, A.R., Shi, G.P., Young, E. and Cox, T.M. (2000) Pathologic gene expression in gaucher disease: up-regulation of cysteine proteinases including osteoclastic cathepsin K. *Blood*, **96**, 1969–1978.
37. Mucci, J.M. and Rozenfeld, P. (2015) Pathogenesis of bone alterations in gaucher disease: the role of immune system. *J. Immunol. Res.*, **2015**, 192761.
38. Boyle, W.J., Simonet, W.S. and Lacey, D.L. (2003) Osteoclast differentiation and activation. *Nature*, **423**, 337–342.
39. Mucci, J.M., Suqueli García, F., de Francesco, P.N., Ceci, R., Di Genaro, S., Fossati, C.A., Delpino, M.V. and Rozenfeld, P.A. (2013) Uncoupling of osteoblast–osteoclast regulation in a chemical murine model of gaucher disease. *Gene*, **532**, 186–191.
40. Mornet, E., Stura, E., Lia-Baldini, A.S., Stigbrand, T., Menez, A. and Le Du, M.H. (2001) Structural evidence for a functional role of human tissue nonspecific alkaline phosphatase in bone mineralization. *J. Biol. Chem.*, **276**, 31171–31178.
41. Sharma, U., Pal, D. and Prasad, R. (2014) Alkaline phosphatase: an overview. *Indian J. Clin. Biochem.*, **29**, 269–278.
42. Orimo, H. (2010) The mechanism of mineralization and the role of alkaline phosphatase in health and disease. *J. Nippon Med. Sch.*, **77**, 4–12.
43. Fujisawa, R. and Tamura, M. (2012) Acidic bone matrix proteins and their roles in calcification. *Front. Biosci. (Landmark Ed)*, **17**, 1891–1903.

44. Young, M.F. (2003) Bone matrix proteins: their function, regulation, and relationship to osteoporosis. *Osteoporos. Int.*, **14**, S35–S42.
45. Baron, R. and Kneissel, M. (2013) WNT signaling in bone homeostasis and disease: from human mutations to treatments. *Nat. Med.*, **19**, 179–192.
46. Bodine, P.V. (2007) Wnt signaling in bone. *IBMS BoneKEy*, **4**, 108–123.
47. Krishnan, V., Bryant, H.U. and MacDougald, O.A. (2006) Regulation of bone mass by wnt signaling. *J. Clin. Invest.*, **116**, 1202–1209.
48. Westendorf, J.J., Kahler, R.A. and Schroeder, T.M. (2004) Wnt signaling in osteoblasts and bone diseases. *Gene*, **341**, 19–39.
49. Doble, B.W. and Woodgett, J.R. (2003) GSK-3: tricks of the trade for a multi-tasking kinase. *J. Cell. Sci.*, **116**, 1175–1186.
50. Verheyen, E.M. and Gottardi, C.J. (2010) Regulation of wnt/beta-catenin signaling by protein kinases. *Dev. Dyn.*, **239**, 34–44.
51. Nusse, R. and Clevers, H. (2017) Wnt/beta-catenin signaling, disease, and emerging therapeutic modalities. *Cell*, **169**, 985–999.
52. Nabavi, N., Urukova, Y., Cardelli, M., Aubin, J.E. and Harrison, R.E. (2008) Lysosome dispersion in osteoblasts accommodates enhanced collagen production during differentiation. *J. Biol. Chem.*, **283**, 19678–19690.
53. Barclay, J.W., Morgan, A. and Burgoyne, R.D. (2005) Calcium-dependent regulation of exocytosis. *Cell Calcium*, **38**, 343–353.
54. Zhao, H. (2012) Membrane trafficking in osteoblasts and osteoclasts: new avenues for understanding and treating skeletal diseases. *Traffic*, **13**, 1307–1314.
55. Castro-Gomes, T., Corrotte, M., Tam, C., Andrews, N.W. and Gasman, S. (2016) Plasma membrane repair is regulated extracellularly by proteases released from lysosomes. *PLoS One*, **11**, e0152583.
56. Andrews, N.W. (2002) Lysosomes and the plasma membrane: trypanosomes reveal a secret relationship. *J. Cell Biol.*, **158**, 389–394.
57. Huynh, C., Roth, D., Ward, D.M., Kaplan, J. and Andrews, N.W. (2004) Defective lysosomal exocytosis and plasma membrane repair in Chediak–Higashi/beige cells. *Proc. Natl. Acad. Sci. USA.*, **101**, 16795–16800.
58. Reddy, A., Caler, E.V. and Andrews, N.W. (2001) Plasma membrane repair is mediated by Ca2+-regulated exocytosis of lysosomes. *Cell*, **106**, 157–169.
59. Jeon, O.H., Panicker, L.M., Lu, Q., Chae, J.J., Feldman, R.A. and Elisseeff, J.H. (2016) Human iPSC-derived osteoblasts and osteoclasts together promote bone regeneration in 3D biomaterials. *Sci. Rep.*, **6**, 26761.
60. Sims, N.A. and Martin, T.J. (2014) Coupling the activities of bone formation and resorption: a multitude of signals within the basic multicellular unit. *Bonekey Rep.*, **3**, 10.1038/bonekey.2013.215.
61. Komori, T. (2010) Regulation of osteoblast differentiation by Runx2. *Adv. Exp. Med. Biol.*, **658**, 43–49.
62. Maor, G., Rencus-Lazar, S., Filocamo, M., Steller, H., Segal, D. and Horowitz, M. (2013) Unfolded protein response in gaucher disease: from human to drosophila. *Orphanet J. Rare Dis.*, **8**, 140.
63. Suzuki, T., Shimoda, M., Ito, K., Hanai, S., Aizawa, H., Kato, T., Kawasaki, K., Yamaguchi, T., Ryoo, H.D., Goto-Inoue, N. *et al.* (2013) Expression of human gaucher disease gene GBA generates neurodevelopmental defects and ER stress in drosophila eye. *PLoS One*, **8**, e69147.
64. Enquist, I.B., Lo Bianco, C., Ooka, A., Nilsson, E., Mansson, J.E., Ehinger, M., Richter, J., Brady, R.O., Kirik, D. and Karlsson, S. (2007) Murine models of acute neuronopathic gaucher disease. *Proc. Natl. Acad. Sci. USA.*, **104**, 17483–17488.
65. Moors, T., Paciotti, S., Chiasserini, D., Calabresi, P., Parnetti, L., Beccari, T. and van de Berg, W.D. (2016) Lysosomal dysfunction and alpha-synuclein aggregation in Parkinson's disease: diagnostic links. *Mov. Disord.*, **31**, 791–801.
66. Du, T.T., Wang, L., Duan, C.L., Lu, L.L., Zhang, J.L., Gao, G., Qiu, X.B., Wang, X.M. and Yang, H. (2015) GBA deficiency promotes SNCA/alpha-synuclein accumulation through autophagic inhibition by inactivated PPP2A. *Autophagy*, **11**, 1803–1820.
67. Schondorf, D.C., Aureli, M., McAllister, F.E., Hindley, C.J., Mayer, F., Schmid, B., Sardi, S.P., Valsecchi, M., Hoffmann, S., Schwarz, L.K. *et al.* (2014) iPSC-derived neurons from GBA1-associated Parkinson's disease patients show autophagic defects and impaired calcium homeostasis. *Nat. Commun.*, **5**, doi:10.1038/ncomms5028.
68. Sun, Y. and Grabowski, G.A. (2010) Impaired autophagosomes and lysosomes in neuronopathic gaucher disease. *Autophagy*, **6**, 648–649.
69. Mazzulli, J.R., Xu, Y.H., Sun, Y., Knight, A.L., McLean, P.J., Caldwell, G.A., Sidransky, E., Grabowski, G.A. and Krainc, D. (2011) Gaucher disease glucocerebrosidase and alpha-synuclein form a bidirectional pathogenic loop in synucleinopathies. *Cell*, **146**, 37–52.
70. Bijsterbosch, M.K., Donker, W., van de Bilt, H., van Weely, S., van Berkel, T.J. and Aerts, J.M. (1996) Quantitative analysis of the targeting of mannose-terminal glucocerebrosidase. predominant uptake by liver endothelial cells. *Eur. J. Biochem.*, **237**, 344–349.
71. Gramlich, P.A., Westbroek, W., Feldman, R.A., Awad, O., Mello, N., Remington, M.P., Sun, Y., Zhang, W., Sidransky, E., Betenbaugh, M.J. *et al.* (2016) A peptide-linked recombinant glucocerebrosidase for targeted neuronal delivery: design, production, and assessment. *J. Biotechnol.*, **221**, 1–12.
72. Tsukimura, T., Tajima, Y., Kawashima, I., Fukushige, T., Kanzaki, T., Kanekura, T., Ikekita, M., Sugawara, K., Suzuki, T., Togawa, T. *et al.* (2008) Uptake of a recombinant human alpha-L-iduronidase (laronidase) by cultured fibroblasts and osteoblasts. *Biol. Pharm. Bull.*, **31**, 1691–1695.
73. Van Patten, S.M., Hughes, H., Huff, M.R., Piepenhagen, P.A., Waire, J., Qiu, H., Ganesa, C., Reczek, D., Ward, P.V., Kutzko, J.P. *et al.* (2007) Effect of mannose chain length on targeting of glucocerebrosidase for enzyme replacement therapy of gaucher disease. *Glycobiology*, **17**, 467–478.
74. Kamath, R.S., Lukina, E., Watman, N., Dragosky, M., Pastores, G.M., Arreguin, E.A., Rosenbaum, H., Zimran, A., Aguzzi, R., Puga, A.C. *et al.* (2014) Skeletal improvement in patients with gaucher disease type 1: a phase 2 trial of oral eliglustat. *Skeletal Radiol.*, **43**, 1353–1360.
75. Lukina, E., Watman, N., Arreguin, E.A., Banikazemi, M., Dragosky, M., Iastrebner, M., Rosenbaum, H., Phillips, M., Pastores, G.M., Rosenthal, D.I. *et al.* (2010) A phase 2 study of eliglustat tartrate (genz-112638), an oral substrate reduction therapy for gaucher disease type 1. *Blood*, **116**, 893–899.
76. Mistry, P.K., Lukina, E., Ben Turkia, H., Amato, D., Baris, H., Dasouki, M., Ghosn, M., Mehta, A., Packman, S., Pastores, G. *et al.* (2015) Effect of oral eliglustat on splenomegaly in patients with gaucher disease type 1: the ENGAGE randomized clinical trial. *JAMA*, **313**, 695–706.
77. Mistry, P.K., Lukina, E., Ben Turkia, H., Shankar, S.P., Baris, H., Ghosn, M., Mehta, A., Packman, S., Pastores, G., Petakov, M. *et al.* (2017) Outcomes after 18 months of eliglustat

therapy in treatment-naive adults with gaucher disease type 1: the phase 3 ENGAGE trial. *Am. J. Hematol*, **92**, 1170–1176.
78. Kahn, M. (2014) Can we safely target the WNT pathway? *Nat. Rev. Drug Discov.*, **13**, 513–532.
79. Garber, K. (2016) Two pioneering osteoporosis drugs finally approach approval. *Nat. Rev. Drug Discov.*, **15**, 445–446.
80. Ishibashi, H., Crittenden, D.B., Miyauchi, A., Libanati, C., Maddox, J., Fan, M., Chen, L. and Grauer, A. (2017) Romosozumab increases bone mineral density in postmenopausal japanese women with osteoporosis: a phase 2 study. *Bone*, **103**, 209–215.
81. Canalis, E. (2018) Management of endocrine disease: novel anabolic treatments for osteoporosis. *Eur. J. Endocrinol.*, **178**, R33–R44.